

The Ultrastructure of Patch-clamped Membranes: A Study Using High Voltage Electron Microscopy

A. Ruknudin, M. J. Song,* and F. Sachs

Department of Biophysical Sciences, State University of New York, Buffalo, New York 14214; and *Wadsworth Center for Laboratories and Research, New York State Department of Health, Albany, New York 12237

Abstract. We have developed techniques for studying patch-clamped membranes inside glass pipettes using high voltage electron microscopy (HVEM). To preserve the patch structure with the least possible distortion, we rapidly froze and freeze dried the pipette tip. The pipette is transparent for more than 50 μm from the tip. HVEM images of patches confirm light microscopy observations that the patch is not a bare bilayer, but a membrane-covered bleb of cytoplasm that may include organelles and cytoskeleton. The membrane that spans the pipette is commonly tens of micrometers from the tip of the pipette and occasionally as far as 100 μm . The structure of patches taken from a single cell type is variable but there are consistent differences between patches made from different cell types. With suction applied to the pipette before

seal formation, we have seen in the light microscope vesicles swept from the plasmalemma up the pipette. These vesicles are visible in electron micrographs, particularly those made from chick cardiac muscle. Colloidal gold labeling of the patch permitted identification of lectin-binding sites and acetylcholine receptors. In young cultures of *Xenopus* myocytes, the receptors were diffuse. In 1-wk-old cultures, the receptors formed densely packed arrays.

The patch pipette can serve, not only as a recording device, but as a tool for sampling discrete regions of the cell surface. Because the pipette has a constant path length for axial rotation, it is a unique specimen holder for microtomography. We have made preliminary tomographic reconstructions of a patch from *Xenopus* oocyte.

THE patch clamp method (Hamill et al., 1981) has revolutionized the study of electrophysiology. Besides making visible the allosteric changes of single-ion channels, the patch clamp has permitted the studies of small and previously inaccessible cells. Despite the flood of papers using patch clamp technology, there is little data concerning patch structure, although one light microscopic study has been recently published (Sokabe and Sachs, 1990). The patch provides a unique opportunity to examine biological structure and function at an unprecedented level of resolution. It is possible, for example, to count the number of channels in a single patch using both electrophysiological and immunocytochemical methods (Ruknudin, A., M. J. Song, A. Auerbach, and F. Sachs, unpublished results). Also, because the patch pipette has axial symmetry, it allows tomographic reconstruction without missing angles. This paper describes techniques for preparing and viewing patches, demonstrates some of the possibilities for imaging, and summarizes our current knowledge of patch ultrastructure.

There are few methods available to study patch ultrastructure. Traditional sectioning procedures are difficult because

the specimen is inside a glass capillary. It would be possible, at least in principle, to embed the tip, etch the glass away with hydrogen fluoride, reembed, and section (Reese, T., personal communication). The process would be both tedious and prone to artifact because of the slow exchange of fixatives and embedding materials within the long and narrow tip. To view the patch as a whole mount inside the pipette using 100–200 keV electron microscopes is not possible because the walls of the pipette are too thick (0.1–1 μm). Scanning EM does not work because the relevant structures are generally deep inside the tip. High voltage electron microscopy (HVEM)¹, however, has the unique ability to penetrate the pipette and image the internal contents with high resolution. We have used the HVEM in both bright- and dark-field modes to study the structure of the patch-clamped membranes.

Materials and Methods

Patch Clamp

We pulled patch pipettes on a Sachs-Flaming pipette puller (model PC-84; Sutter Instruments, San Rafael, CA) using borosilicate capillaries (100- μl

1. *Abbreviations used in this paper:* AChR, acetylcholine receptor; HVEM, high voltage EM.

Preliminary accounts of some of this work have appeared in abstract form (1987. *Biophys. J.* 51:517; 1989. *Proc. Electron. Microsc. Soc.* 47:936–937).

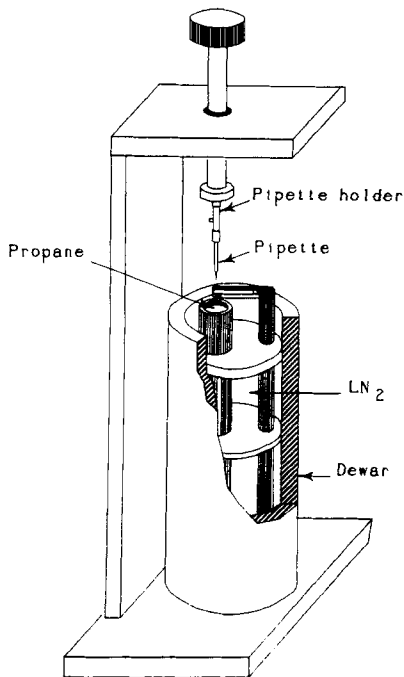


Figure 1. Freeze-fixing apparatus. The pipette holder was mounted in a rod suspended in linear ball bearings and held up by a magnet. After inserting the holder, the vertical rod was pushed down immersing the tip in cold propane held in a cup in the central rod. The figure shows a tip cassette held in a second cooled aluminum rod. Bar, 10 cm.

Microcaps; Drummond Scientific Co., Broomall, PA). To minimize wall thickness, the pipettes were not fire polished and had resistances of 2–10 M Ω when filled with normal saline. EM showed tip openings of 0.5–2.0 μ m. We made patches in the standard manner by applying suction (5–50-mm Hg depending upon cell type) to draw a bleb of membrane into the pipette (Hamill et al., 1981).

Channel activity served as an indication of patch integrity. Stretch-activated channel activity was evoked by applying pulses of suction to the pipette, both before and after excision from the cell. Nicotinic acetylcholine

receptor (AChR) channels were activated by including 100 nM acetylcholine in the pipette solution.

After making a seal and verifying patch integrity, we excised the patch from the cell for freezing or labeling with antibodies. To protect the patch from dehydration during transfer from the recording medium, we covered the tip of the pipette with a sleeve of Teflon tubing (12 mm long; 1.6-mm inner diameter) (Quartararo and Barry, 1987). The sleeve, which had a constriction to prevent it from slipping, was slipped over the back of the pipette before inserting the pipette into the electrode holder. Control pipettes were handled in exactly the same way as those containing patches: filling, insertion into the recording chamber, removal for freezing, etc. The only difference was that the control pipettes were brought near the cells, but never touched them.

Freeze Fixation

The electrode holder could be quickly removed from the micromanipulator while maintaining pressure on the pipette. After removing the holder, we placed it in the freeze-fixing device shown in Fig. 1. Pushing back the protective sleeve, we plunged the pipette into liquid propane cooled by liquid nitrogen.

Freeze Drying

While keeping the tip of the pipette in propane, we separated the pipette holder from the shaft of the freezer, and slipped the frozen pipette tip under a spring clip into a groove in a precooled aluminum cassette (Fig. 2 A). We then broke off the back of the pipette using a microfile, leaving the final 1 cm protected in the cassette. The cassette was transferred to a precooled "holding plate" (Fig. 2 B) that stored six cassettes. The plate, in turn, was stored in an aluminum box cooled with liquid nitrogen until ready for dehydration.

When a group of samples was ready for drying, we transferred the holding plate to a modified cold stage in a BA 510 equipped with a GA1 freeze-etching unit (Balzers, Hudson, NH). We replaced the original stage with a 6 \times 9-cm aluminum plate and precooled it to -146°C under vacuum before inserting the samples to be dried. When breaking vacuum, we vented with dry N₂ to reduce condensation. The holder plate was removed from a dewar of liquid-nitrogen and clamped to the cold stage; the bell jar was closed and the chamber evacuated immediately. Within 2 min, the pressure fell to 10^{-6} mbar and the temperature returned to -146°C . Within 30 min the vacuum reached 4×10^{-7} mbar. Using a homebuilt temperature programmer, we raised the temperature of the cold stage $1^{\circ}\text{C}/\text{min}$ to -130°C , and then $0.05^{\circ}\text{C}/\text{min}$ to -120°C . During this period, the pressure rose to 6×10^{-6} mbar and then returned to 10^{-7} mbar. From -120°C , we raised the temperature $1^{\circ}\text{C}/\text{min}$ to reach room temperature and left the pipette tips in vacuum overnight.

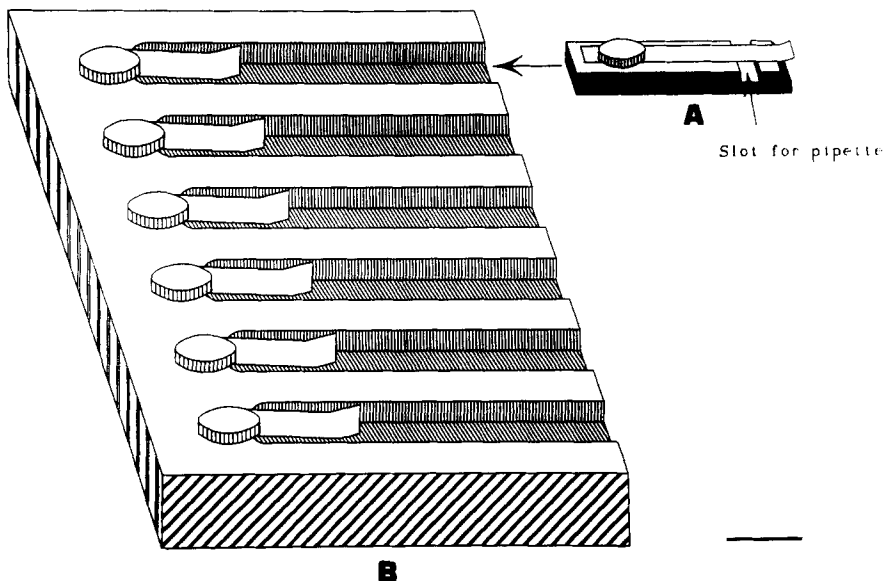


Figure 2. Cassette (A) and cassette holder (B). Bar, 1 cm.

Mounting the Tip

The next day, we took the holder plate from the vacuum chamber and, if appropriate, exposed it to osmium tetroxide vapor in a sealed, desiccated, vessel for 5–10 min. Mounting the pipette tip on a conventional single-hole grid required that we glue the final 1.5 mm of the tip to the grid. We placed a tiny drop of UV curing glue (Loctite Corp., Cleveland, OH) on the grid and then, holding the pipette with forceps mounted on a micromanipulator, centered the tip and pressed it into the glue. With a UV gun (Electro-lite Corp., Danbury, CA) we catalyzed the glue in ~20 s. Scoring the pipette at the edge of the grid with a diamond microfile held in a second micromanipulator, we snapped off the tip by bending the pipette shaft. This stage of the processing was susceptible to rehydration and we attempted to keep the laboratory below 20% relative humidity. After mounting, the grids were coated with 100–150 nm carbon by electron beam evaporation to prevent charging (models EVM052 and QSG201; Balzers) and were stored in a desiccator.

Preparation of Cultures

Xenopus Myocytes. The isolation procedure followed that of Kidokoro et al. (1980). Briefly, somites from stage 18–21 *Xenopus laevis* embryos were separated from surrounding yolk, notochord and spinal cord by microdissection and incubation in a low Ca^{2+} -collagenase (1 mg/ml; type 1A; Sigma Chemical Co., St. Louis, MO) solution. We dissociated myocytes from somites by incubation in a divalent cation-free saline containing trypsin (0.05 mg/ml; Gibco Laboratories, Grand Island, NY). We maintained the cultures for 1–7 d at room temperature in 60% (vol/vol) Liebovitz L-15 medium containing 8 mM Hepes, 0.5% (vol/vol) heat-inactivated horse serum, and 1 $\mu\text{g}/\text{ml}$ gentamycin. For patch clamping, we replaced the culture medium with saline containing 100 mM NaCl, 1.6 mM KCl, and 10 mM Hepes, pH 7.4, and filled the pipettes with the same solution.

Xenopus Oocytes. Preparation of oocytes for patch clamping followed the procedure of Mishina et al. (1986). Briefly, we removed portions of ovary from mature frogs, placed them in Barth's medium and stored them in a refrigerator at 10°C (usually for a few days). On the day of the experiment, we incubated pieces of ovary in 1 mg/ml collagenase (type 1; Sigma Chemical Co.) in a shaker to free the oocytes from the ovary. After dissecting the follicle cells, we put the individual oocytes in a hypertonic "stripping" solution to separate the vitelline membrane from the oocytes and removed it with sharpened No. 5 forceps. For patch clamping, the bath and pipette contained *Xenopus* Ringer's solution.

Chick Skeletal Myotubes. The preparation followed the procedure of Guharay and Sachs (1984). We removed pectoral muscles from 11-d-old White Leghorn embryos using sterile techniques, dissociated them in divalent ion-free saline containing collagenase (1 mg/ml, type 1A; Sigma Chemical Co.), and plated the myoblasts in 60-mm plastic culture dishes containing polylysine-coated coverslips at a density of $\sim 10^6$ cells/dish. We grew the cells in DME supplemented with 10% (vol/vol) heat-inactivated horse

serum, 2% (vol/vol) embryo extract, penicillin, and streptomycin, in an atmosphere of 95% relative humidity at 37°C containing 5% CO_2 air. After 2–3 d in culture, we treated the cells for 24–36 h with medium containing 10^{-5} M cytosine arabinoside to reduce fibroblast growth (Fischbach, 1972). The bath and pipette contained normal saline (150 mM NaCl, 5 mM KCl, 2 mM CaCl_2 , 1 mM MgCl_2 , and 10 mM Hepes, pH 7.4).

Chick Cardiac Myocytes. Hearts from 10–12-d embryos were removed, trimmed of the great vessels, cut into small pieces, and then dissociated and cultured according to the procedure described above for chick skeletal muscle, except that cytosine arabinoside was omitted.

Astrocytes. Glial cells were isolated from cerebral cortices of neonatal rats according to the dispase-dissociation method of Frangakis and Kimelberg (1984) and grown in BME plus 10% FCS (Gibco Laboratories). Bath and pipette contained Hepes-buffered Ringer's solution containing 122 mM NaCl, 3.8 mM KCl, 1.3 mM CaCl_2 , 0.4 mM MgCl_2 , 10 mM glucose, and 25 mM Hepes, pH 7.4. For making outside-out patches, the pipette contained 10 mM KCl, 100 mM KF, 10 mM KEGTA, 10 mM Hepes, 1 mM MgSO_4 . A seal was formed in the normal way and the patch was then broken with strong suction forming a whole-cell clamp. The pipette was then withdrawn from the cell forming a neck of membrane that pinched off to form a patch with the extracellular surface facing the bath.

Immunocytochemical Staining

We labeled the extracellular surface by including gold-conjugated lectins such as *Dolichos bifloru* agglutinin in the pipette or preincubating the cells with lectin-gold complexes such as Con A-horseradish peroxidase-gold (E.Y. Laboratories, Inc., San Mateo, CA). When we included labels in the pipette-filling solution, we did not wash out the nonspecifically bound particles. The gold simply served as a marker of the extracellular side of the membrane. We labeled AChRs with colloidal gold by the following method. After excision, we fixed the inside-out patch in 0.25% formaldehyde, washed it with PBS, and incubated the patch in PBS containing 1% BSA. We then incubated the tip with primary antibodies (100 nM) made against the cytoplasmic side of the β subunit of *Torpedo* AChR (mAb 111 courtesy of J. Lindstrom). The primary antibodies were then labeled with anti-rat secondary antibodies conjugated with 10-nm colloidal gold (Janssen Pharmaceutica, Beerse, Belgium). We then rinsed the tip with PBS and froze it. Controls consisted of omitting the primary antibodies. Microtomographic reconstructions were made according to standard procedures (Frank et al., 1987; McEwen, B. F., M. J. Song, A. Ruknudin, D. P. Barnard, J. Frank, and F. Sachs, unpublished procedures) at 2° increments between -64° and 66° tilt angles.

Results

Fig. 3 shows a saline-filled control pipette, processed through freeze fixing and freeze drying, under bright-field illumina-

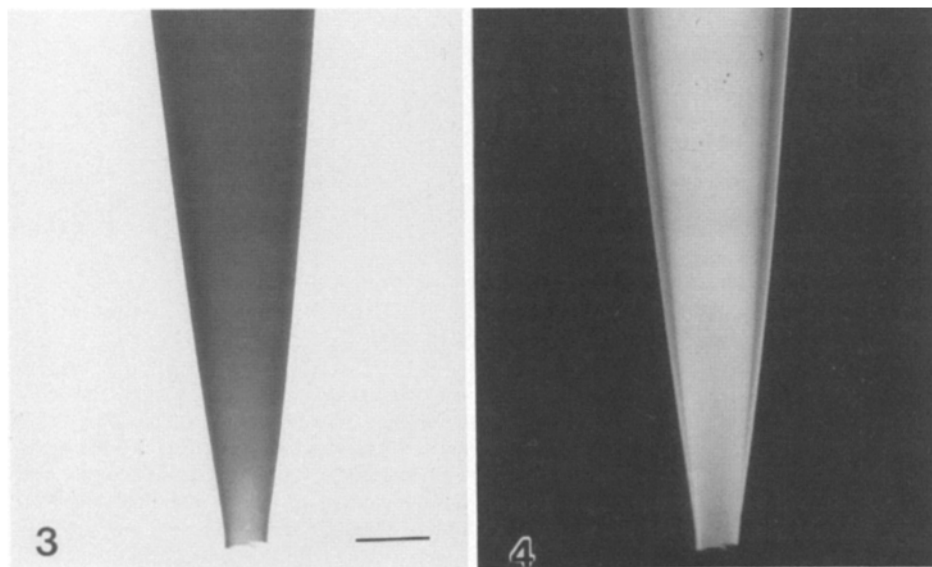


Figure 3 and 4. A saline-filled control pipette processed along with patch-clamped pipettes. Fig. 3 is a bright-field image and Fig. 4 is a dark-field image of the same pipette. The bright-field image does not reveal the inside of the pipette completely whereas the dark-field image provides details over a long region of the pipette. Note that the contrast is not completely reversed in the two images. In the dark-field image, some of the pipette is dark, as it is in the bright-field image. Bar, 2 μm .

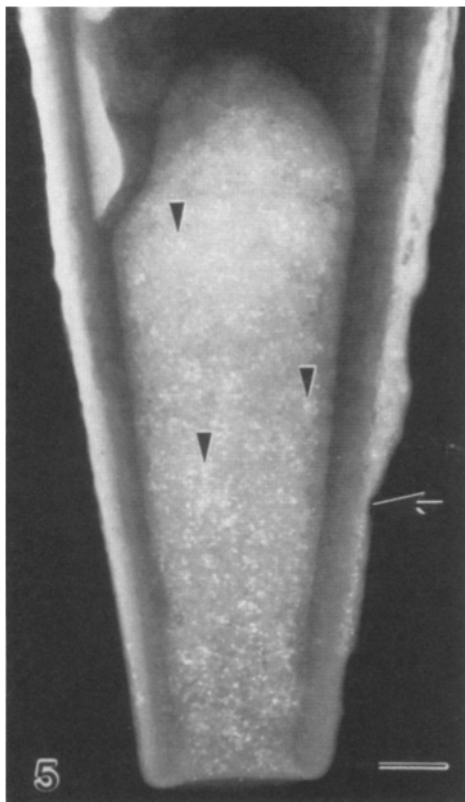


Figure 5. Dark-field image of a patch from chick skeletal myotube. The cell was labeled with Con A followed by HRP-gold (15 nm) before the patch was made. Note the classical Ω shape. The gold particles are seen as white dots (arrowheads show representative particles) coating the interior walls of the pipette up to the dome. Arrow shows shreds of membrane with adhering cytoplasm that stick to the outside of the patch pipette after excision. Above the dome is a dense amorphous material that is probably extracellular matrix. Bar, 0.5 μm .

tion. Under these exposure conditions, the tip is transparent but most of the remainder is dark. Because of the increase in wall thickness with distance from the tip, it is difficult to view a long expanse of the pipette with a single bright-field exposure. However, under dark-filled illumination the interior is visible over a much longer expanse of tip (Fig. 4). The cleanliness of these control pipettes shows that the structures observed in membrane-containing pipettes come from the membranes themselves, not from some artifact associated with immersion in the recording media or with the preparation technique.

In the light microscope, patch formation is visible in real time. Generally the membrane moves slowly into the pipette and then sticks to the wall to form a gigohm seal (Sokabe and Sachs, 1990). The resulting patch often looks like an Ω in the pipette tip (Sakmann and Neher, 1983). Fig. 5 is the dark-field image of a "classical" patch made from chick skeletal muscle. We labeled the extracellular side of the membrane with Con A bound to a secondary protein horseradish peroxidase-conjugated with gold. The colloidal gold particles appear as white dots. Membrane coats the inner walls of the pipette for $\sim 4 \mu\text{m}$ from the tip. The dark material above the seal region is presumably basement mem-

brane, but is not clearly resolved by HVEM under these conditions. Membrane has also stuck to the outside of the pipette. When the patch is excised, flaps of torn membrane often stick to the outer wall. It was possible to form a gigaseal even with this high density of large gold particles (15 nm) suggesting that the seal is distributed rather than punctate. The fact that the gold particles are covering the whole patch membrane suggests that they are not free to diffuse and probably tied to cytoskeleton, for otherwise we might expect them to get caught on the edge of the pipette tip, concentrated there, and depleted from the patch. This classical Ω -shaped patch proved to be surprisingly uncommon. There were wide variations from patch to patch even when we made them from a single cell type. But beyond this variability we saw also consistent differences in structure between patches made from different cell types.

Types of Patches Based on Their Morphology

Though we followed a standardized procedure to make the pipettes and the seals, we saw two general types of patch structure. When the pipette-spanning membrane (the "dome") formed near the tip, there was a continuous coat of membrane along inner wall of the pipette. The continuity of membrane was clear when we labeled the plasmalemma with lectin-gold was shown in Fig. 5. Fig. 6 shows one of these patches having cytoplasmic material and filaments distributed in the tip region. The dome lies far above the region shown.

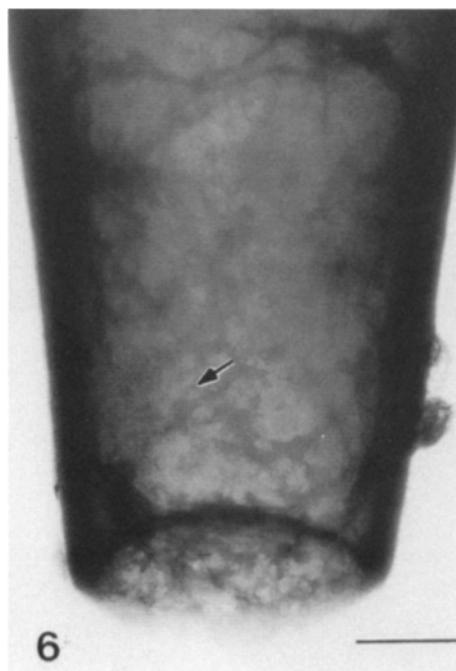


Figure 6. A patch made from *Xenopus* skeletal myocyte. The cytoplasmic fibrous material is distributed in the tip. The dome is far above the region shown. Membrane adheres closely to the inner wall of the pipette (most readily visible in stereo images, not shown). Arrow indicates a group of gold particles attached to AChRs in the membrane. Bar, 0.5 μm .

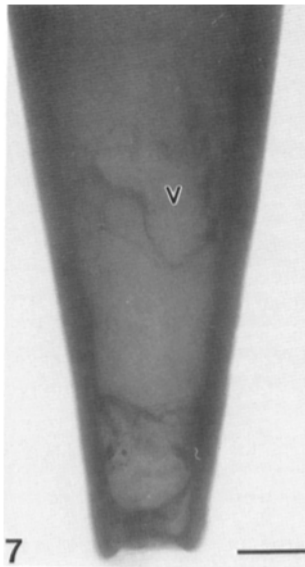


Figure 7. Membrane vesicles (V) in a patch made from chick skeletal myotube. The dome membrane is probably at the tip of pipette. Vesicles are large (1-2 μm) and they do not possess any visible internal organization. Bar, 1 μm .

Some pipette tips contained membrane vesicles. The vesicles, without cytoplasmic material, sometimes appeared to be on the intracellular side of the patch membrane (Fig. 7). In other cases, particularly with chick cardiac muscle, the vesicles were on the extracellular side of the patch (Fig. 8). These vesicles formed when we applied suction before seal formation. Shear stress from the flow of water over the cell surface pulled plasmalemmal tethers up the tip where they pinched off the formed vesicles. These observations raise questions about the significance of electrical recordings made from these patches. The membrane that originally lay beneath the pipette tip formed the electron-lucent vesicles that now lie above the patch. The membrane that actually formed the patch may have come from new plasmalemma that flowed in, from fusion of the vesicles (as sometimes ob-

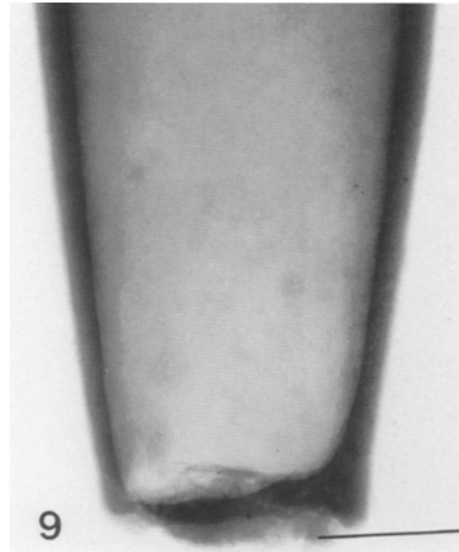


Figure 9. An inside-out patch made from a *Xenopus* myocyte showing the membrane seal region at the extreme tip of the pipette. We saw no other cytoplasmic structures in this pipette. Bar, 0.5 μm .

served in the light microscope), or even from intracellular organelles. Further experiments with labeled membranes are necessary to resolve the issue. With the chick heart cells, the patch always formed close to the tip and the patch membrane appeared extraordinarily dense (Fig. 8). Notice that in Fig. 8 the patch region appears as dense as the walls of the pipette. Unlike the patches from cardiac myocytes, patches made from *Xenopus* myocytes have thin membranes and sometimes appear at the extreme end of the pipette (Fig. 9).

Often the dome was found far from the tip (Fig. 10). In Fig. 10, the dome structure was 25 μm from the tip, but we have found similar structures as far as 100 μm from the tip.

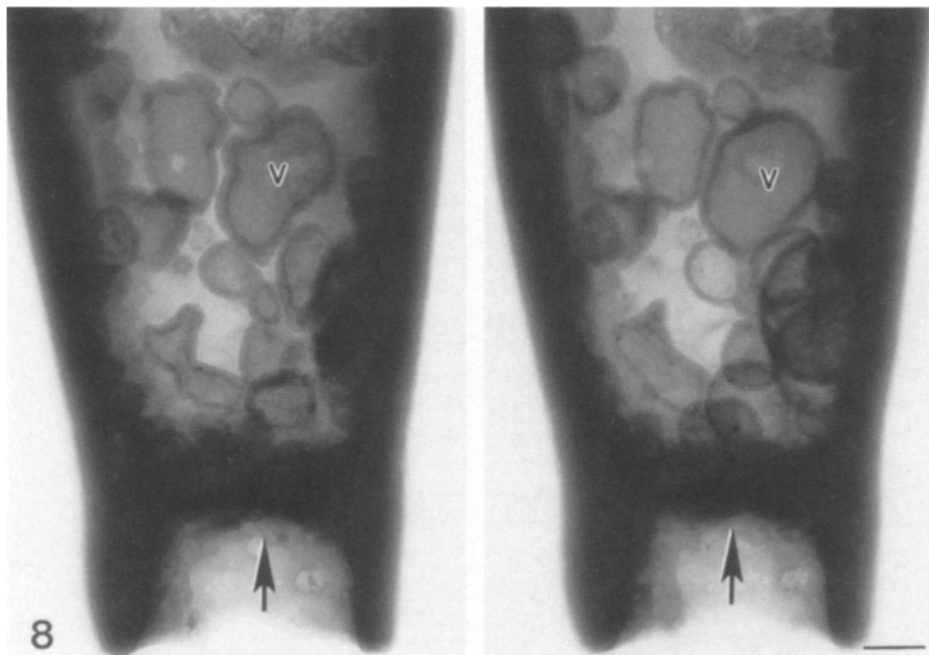


Figure 8. Stereo view of a patch prepared from a chick cardiac myocyte. The arrow points to the dome located close to tip of the pipette. Numerous membrane vesicles (V) are seen above the dome. Notice the electron-dense membrane. Below the dome region, the membrane coating the interior of the pipette has lighter spots that may represent lipid phase transitions or intramembrane particles. Tilt angle 6°. Bar, 0.25 μm .

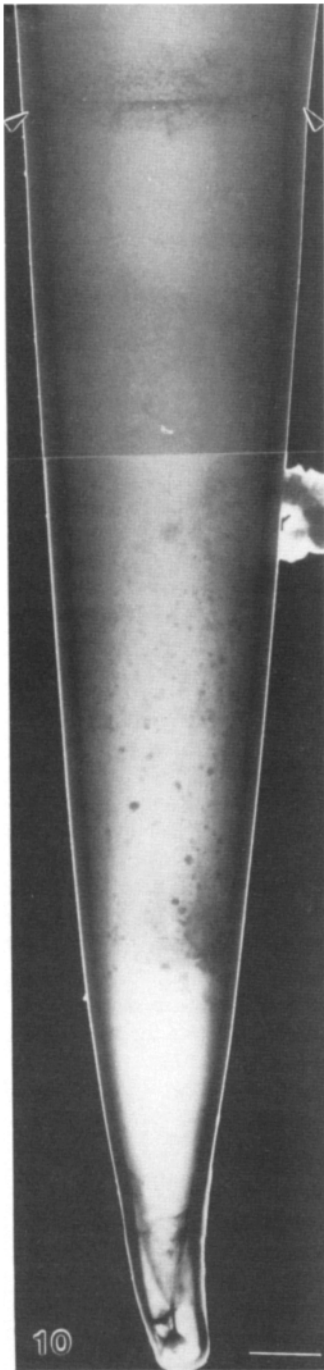


Figure 10. A dark field view of the pipette made from *Xenopus* myocyte. Arrows indicate the dome that was probably the electrically limiting membrane. Gold labels for AChR were located up to, but not beyond this region. This is a common kind of patch with the dome located high in the pipette. Bar, 2.5 μm .

In fact, in the beginning of the study we often threw away samples when we did not find a patch in the tip, believing that the patch had broken (which might have sometimes been true). Only when we began using dark-field microscopy did we find intact, pipette-spanning domes far from the pipette tip. The dome region is formed by a membrane (dark line) with attached fibers. This is consistent with many light microscopic images that show a patch to consist of a membrane-covered plug of cytoplasm that can travel as a unit up the pipette (Sokabe and Sachs, 1990). Although the image of Fig. 10 looks like a rim of disrupted cytoskeleton, the membrane is actually intact as can be seen in stereo images

and in reconstructions. Fig. 11 is a stereo image of another patch of *Xenopus* oocyte some 30 μm up the pipette. The patch membrane with attached cytoskeletal filaments spans the interior walls of the pipette. There is some material that could be deposits of salts from the buffer. In collaboration with Drs. B. F. McEwen and J. Frank of Wadsworth Laboratories, New York State Department of Health, Albany, we made a tomographic reconstruction of this patch (McEwan, B. F., M. J. Song, A. Kuknudin, D. P. Bernard, J. Frank, and F. Sachs, unpublished procedures). We took the volume image ($\sim 250 \text{ px}^3$), operated on it with a three-dimensional gradient operator and rendered the resulting image. A stereo pair from that reconstruction is shown in Fig. 12. Fibrous material adheres to the interior walls of the pipette for $\sim 1 \mu\text{m}$ down from the dome. Fibrous cytoskeletal structures also span the pipette. The lipid membrane of Fig. 11 lies above this mat of cortical cytoskeleton. We plan to identify specific components of this meshwork using immunogold labeling.

Outside-out Patches. We made outside-out patches from rat astrocytes. In some pipettes the membrane could be clearly seen to span the tip (Fig. 13). This micrograph also shows elaborate cytoplasmic and membranous structures behind the tip-most membrane. Other patches showed more complicated, irregular patch structure that appeared to reflect folding of excess membrane in the tip region. Some outside-out patches showed dense cytoplasm extending for 20 μm or more back of the patch membrane (Fig. 14).

AChR Channels. We identified AChR channels in *Xenopus* myocytes with monoclonal antibodies and colloidal gold. In myocytes on the first day in culture, we found the AChRs distributed over wide areas of membrane (Fig. 15). The average density along the pipette walls was $\sim 40/\mu\text{m}^2$, but the distribution varied widely from patch to patch, ranging from ~ 2 to $100/\mu\text{m}^2$. In myoblasts cultured for 7 d, the AChRs aggregated (Fig. 16) into polygonal patches containing ~ 50 gold particles with a peak density of $\sim 3,000/\mu\text{m}^2$. The peak density may be limited by the steric interaction of the colloidal gold particles rather than the true receptor density.

Discussion

We have described techniques for studying the ultrastructure of patch-clamped membranes presented the initial results. Rapid freezing of the pipette should preserve the structure of the patch as closely as possible to that which existed when we made the electrical recordings. We saw no obvious evidence of ice crystal formation even when membranes were 100 μm from the tip. The pipette has a thermal diffusion distance of only a few micrometers and the specific heat of the glass is small relative to water. The cytoplasmic material that we saw attached to the patch membrane resembled images of cytoplasm seen in whole cells after cryopreservation (Porter and Anderson, 1982; Bridgman et al., 1986). Cryopreservation can even produce images of unsupported lipid membranes (Crowe et al., 1987). Recently, Linner et al. (1986) have shown that freeze drying at lower temperatures improves preservation of the fine structure. Following their lead, we freeze dried our specimens near -128°C .

The distance between the pipette-spanning dome and the tip seemed to increase with the amount of suction applied to

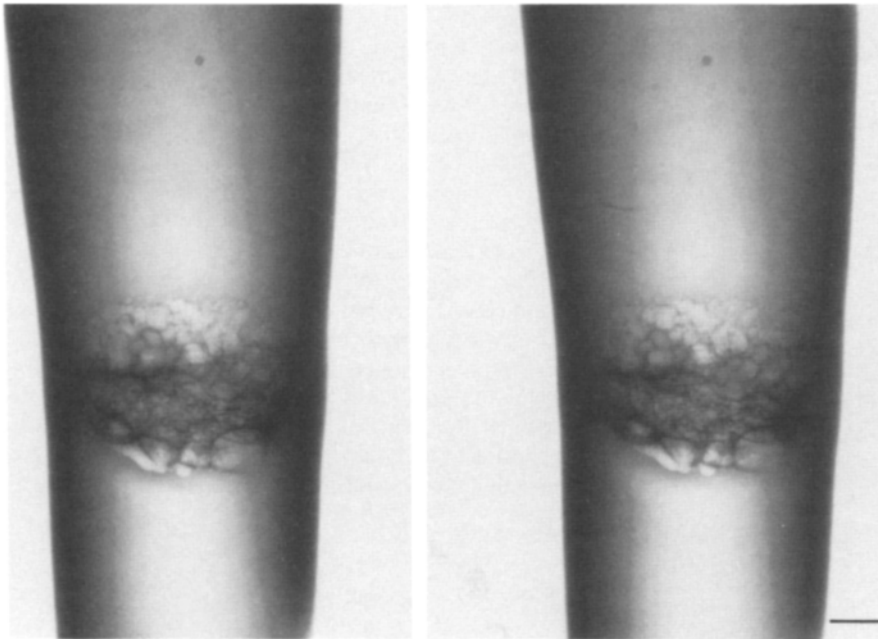


Figure 11. Stereo pair of the dome structure of a patch from *Xenopus* oocyte located 35 μm from the pipette tip. The patch has separated from other structures near the tip but clearly spans the pipette. Tilt angle 6°. Bar, 1.0 μm .

form a seal. When we formed patches using suction by mouth, the domes were at a greater distance from the tip than ones formed with slow controlled suction using mechanical devices. The properties of the tissue clearly had some influence on the location of the patch. Patches from chick heart cells always formed within 5 μm of the tip while those from other tissues formed 10–20 μm or more from the tip. Post et al. (1988) suggested that based on phospholipid composition of cardiac sarcolemma, the inner monolayer of the membrane is unstable and easily disturbed upon exposure to high calcium. Upon excision, the sarcolemma of chick heart cells could have undergone a phase transition to form the dense dome region. More likely, however, is that the membranes are convoluted and covered with a dense extracellular matrix.

The membrane binds tightly to the glass as necessary to account for the high resistance of the seal (Hamill et al.,

1981). We can't measure the distance between the membrane and the glass since the pipette wall is too thick and conceals details perpendicular to the axis of the pipette. We are now developing freeze-fracture techniques that may clarify these details. The seal itself is most likely a distributed rather than discrete structure since we could make good seals even when the extracellular surface was heavily labeled with 40-nm colloidal gold.

We found that in many patches the dome was not clearly distinguished. This may have occurred because the dome was thin and located in a thick region of the pipette, or because the membrane was broken, either before freezing or afterward as a result of accidental rehydration and dehydration. When visible, the bilayer membrane in the dome region could be seen as a thin veil (Fig. 10) best seen in stereo pairs (Fig. 11). When the plane of the membrane lay normal to the viewing direction, it was possible to see a trilaminar struc-

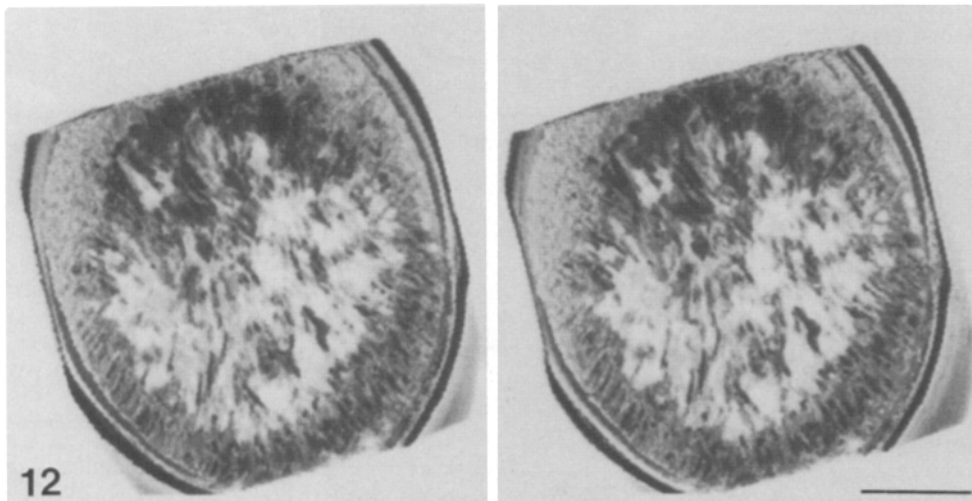


Figure 12. Tomographic reconstruction of the patch shown in Fig. 11. Stereo view was made from the voxel data set after treatment with a three-dimensional gradient operator and rendering. Although exaggerated in density by the gradient operator, there are cytoskeletal fibers stuck to the inner walls and spanning the pipette. The lipid membrane is not visible in the reconstruction because of its low density but is visible in the original images as a thin veil overlying the meshwork.

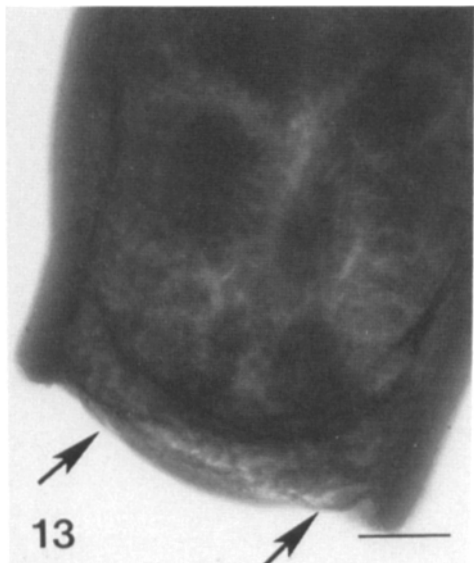


Figure 13. An outside-out patch made from rat astrocyte. A membrane dome spans the tip of the pipette (arrows), but since there is more than one membrane-like structure in the tip, we cannot tell which one is the electrically limiting. The cytoplasmic structures above the membranes are not clear in this bright-field image. Bar, 0.5 μm .

ture. In nearly all cases we saw the interior pipette walls covered with membrane. This membrane contained round, light spots which may represent regions of lipid phase separation or perhaps areas of membrane collapse around integral membrane proteins (Fig. 8). These spots resembled the pits observed during fusion of lipid membranes (Verkleij et al., 1985).

The dome membrane was always supported by fibrous elements. These fibers looked similar to membrane cytoskeleton seen in platelets and erythrocytes (Ohtake, 1986). Wall and Patel (1989) have shown cytoskeletal fibers attached to the plasma membrane of *Xenopus* oocytes and Giebelhaus et al. (1987) have demonstrated spectrin-based cortical cytoskeleton. Steiner et al. (1989) have shown that β -spectrin associates with a membrane protein of brain synaptosomes and they suggested that this membrane protein could be a channel protein. There is evidence that ankyrin links the voltage-dependent sodium channels to the underlying spectrin cytoskeleton in rat brain (Srinivasan et al., 1988). By extending the current studies with specific labeling of the cytoskeleton, we will be able to identify specific cytoskeletal proteins in individual patches. Double-label experiments using cytoskeletal and receptor tags would be particularly helpful in understanding the specific associations.

Using antibodies from clone 111b (courtesy of J. Lindstrom) we found the AChRs in the patch were distributed similarly to the way they distribute in vivo (Sargent et al., 1984). In young cells (a few days) the receptors tended to occur with a relatively low density ($2\text{--}100/\mu\text{m}^2$), but in older cells (1 wk) they tended to form dense clusters ($3,000/\mu\text{m}^2$) similar to those described in rat myocytes (Vetzel and Robenek, 1988). At the motor end plate, Matthews-Bellinger and Salpeter (1978) estimated that the channel density was $\sim 10,000/\mu\text{m}^2$. In other regions of the muscle, the AChR

density is much less. For example, in developing rat skeletal muscle (16-d embryos), the receptor density is ~ 130 sites/ μm^2 (Bevan and Steinback, 1977). Sometimes receptors in the patch were neither clustered nor uniformly distributed, but followed what appeared to be some component of the cytoskeleton. Recently, Bloch and Morrow (1989) demonstrated that clustered AChRs in rat myotubes are closely linked to β -spectrin.

Since patches may contain a small number of ion channels, it is possible to compare the number of active channels estimated from electrical measurements with the number of receptors observed with immunogold labeling. It is possible to accurately count receptors using immunogold cytochemistry provided that the gold particles are not too large (Griffiths and Hoppeler, 1986; Gu and D'Andrea, 1989). The results presented here and in the earlier paper of Sokabe and Sachs (1990) show that it is possible to combine electrophysiology,

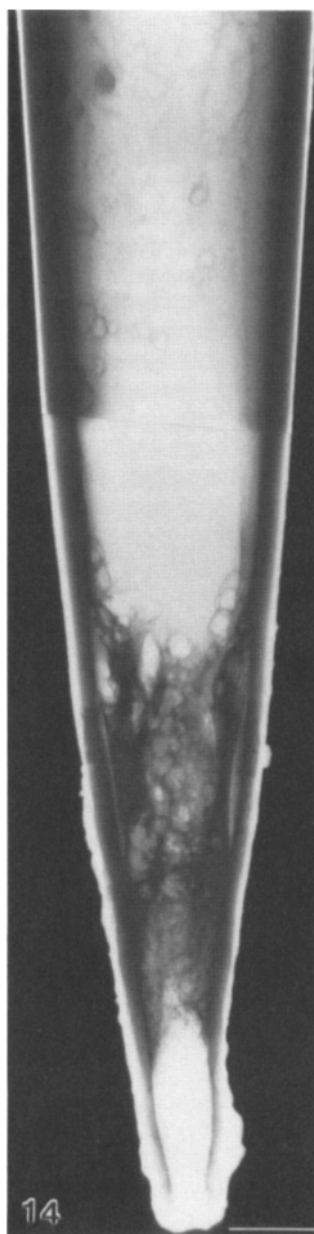


Figure 14. A dark-field image of an outside-out patch prepared from a rat astrocyte. Note the large amount of cytoplasmic material in the pipette. The regions above and below the cytoplasmic mass are overexposed showing the nonmonotonic relationship between electron density and brightness in dark field. Bar, 2 μm .

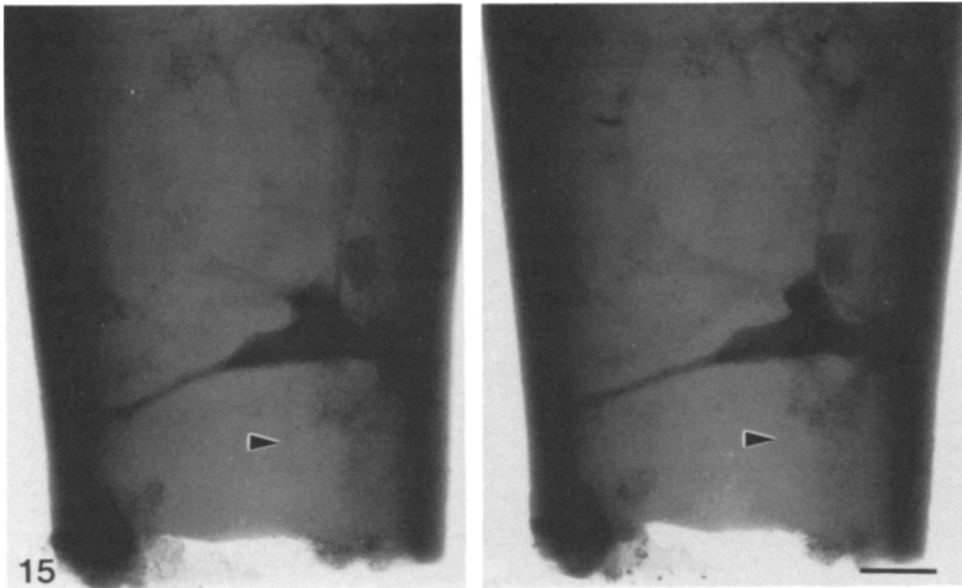


Figure 15. A bright-field stereo pair of a patch made from a *Xenopus* myocyte (1 d in culture) and stained for AChRs (arrows) showing diffuse but not random location of the receptors in a young myotube. The pipette spanning structures appear to be condensed cytoplasm. Tilt angle 10°. Bar, 0.25 μm .

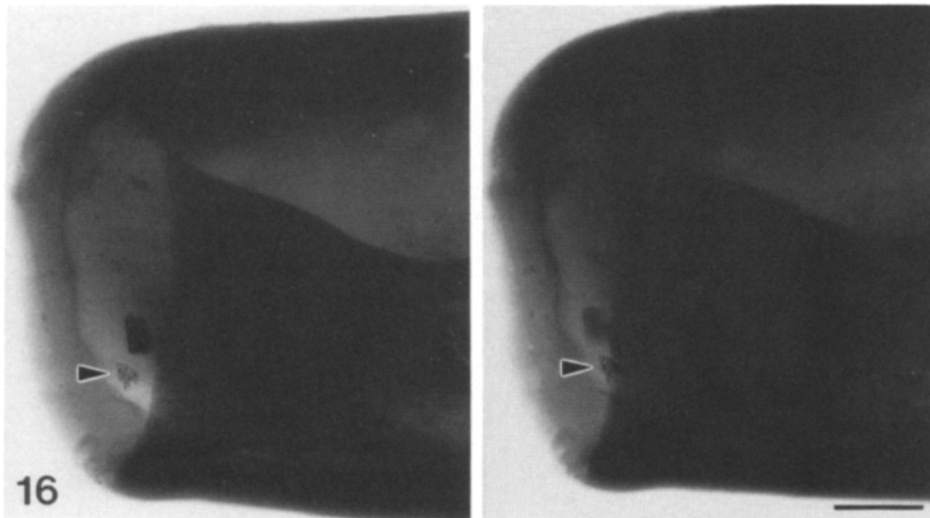


Figure 16. Stereo pair of a patch from a 7-d *Xenopus* myocyte. The membrane forms a funnel attached at its wide end to the pipette tip. Above this region, the membrane reexpanded to contact the walls and form the dome (not shown). Note the compact clusters of AChRs (arrows) marked by 10-nm gold particles and compare this with the relatively diffuse distribution shown in Fig. 15. This pipette was fire polished before making a seal. Bar, 0.5 μm .

light microscopy, and EM on the same patch. We have not yet studied the same patch under both high resolution light microscopy and EM because the pipette-holding system for high resolution light microscopy is too cumbersome for rapid freezing. We are now building a new pipette freezer that will permit such studies. Comparisons between light and electron microscopic images of the same patch will help to identify structures that are readily visible in only one modality, i.e., fluorescently labeled mitochondria, and will help to clarify any artifacts occurring in the preparation of specimens for the HVEM.

The pipette has proven to be a unique sample holder for EM. It can be rotated axially 360° with a constant path length and $\sim\pm 70^\circ$ in azimuth. Taking advantage of these wide degrees of freedom we have made preliminary tomographic reconstructions (Frank et al., 1987) of a patch with a resolution of ~ 300 nm (McEwen, B. F., M. J. Song, A. Ruknudin, D. P. Barnard, J. Frank, and F. Sachs, unpub-

lished procedures). Since the resolution (for the same number of images) is inversely proportional to the dimensions of the sample, with smaller pipette tips and with patches carefully kept to the tip region, the resolution of a patch could be increased to ~ 50 nm using ~ 100 images. Although tedious, the highest accuracy images should come from working on a cryostage and keeping the patches frozen instead of drying them. By sealing shut the tip, the pipette becomes a sample holder for organelles, and if the back is sealed it may be used as a microhydration chamber to view wet, possibly moving, samples. Since pipettes can be made with diameters < 20 nm, they may serve as sample holders for low dose structural analysis of molecular structure with no limitation on tilt angle.

This work was supported by the Muscular Dystrophy Association, grant DK 37792-10 from the U.S. Public Health Service, and grant LS-22560 from the United States Army Research Office to F. Sachs, and by Biotech-

nological Resource Grant RR01219 from the division of research resources, Department of Health and Human Services/Public Health Service to NYS HVEM facility at Albany, NY.

Received for publication 9 February 1990 and in revised form 14 September 1990.

References

- Bevan, S., and J. H. Steinbach. 1977. The distribution of α -bungarotoxin binding sites on mammalian skeletal muscle developing in vivo. *J. Physiol. (Lond.)* 267:195-213.
- Bloch, R. J., and J. S. Morrow. 1989. An unusual β -spectrin associated with clustered acetylcholine receptors. *J. Cell Biol.* 108:481-493.
- Bridgman, P. C., B. Kachar, and T. S. Reese. 1986. The structure of cytoplasm in directly frozen cultured cells. II. Cytoplasmic domains associated with organelle movements. *J. Cell Biol.* 102:1510-1521.
- Crowe, J. H., B. J. Spargo, and L. M. Crowe. 1987. Preservation of dry liposomes does not require retention of residual water. *Proc. Natl. Acad. Sci. USA.* 84:1537-1540.
- Fischbach, G. D. 1972. Synapse formation between dissociated nerve and muscle cells in low density cell cultures. *Dev. Biol.* 28:407-429.
- Frangakis, M. V., and H. K. Kimelberg. 1984. Dissociation of neonatal rat brain by dispase for preparation of primary astrocyte cultures. *Neurochem.* 9:1685-1693.
- Frank, J., B. F. McEwen, M. Radermacher, J. N. Turner, and C. L. Rieder. 1987. Three-dimensional tomographic reconstruction in high voltage electron microscopy. *J. Electron Microsc.* 6:193-205.
- Giebelhaus, D. H., B. D. Zelus, S. K. Henchman, and R. T. Moon. 1987. Changes in the expression of α -fodrin during embryonic development of *Xenopus laevis*. *J. Cell Biol.* 105:843-853.
- Griffiths, G., and H. Hoppeler. 1986. Quantitation in immunocytochemistry: correlation of immunogold labeling to absolute number of membrane antigens. *J. Histochem. Cytochem.* 34:1389-1398.
- Gu, J., and M. D'Andrea. 1989. Comparison of detecting sensitivities of different sizes of gold particles with electron microscopic immunogold staining using atrial natriuretic peptide in rat atria as a model. *Am. J. Anat.* 185:264-270.
- Guharay, F., and F. Sachs. 1984. Stretch-activated single ion channel currents in tissue-cultured embryonic chick skeletal muscle. *J. Physiol. (Lond.)* 352:685-701.
- Hamill, O. P., A. Marty, E. Neher, B. Sakmann, and F. J. Sigworth. 1981. Improved patch-clamp techniques for high-resolution current recording from cells and cell-free membrane patches. *Pflugers Arch. Eur. J. Physiol.* 391:85-100.
- Kidokoro, Y., M. J. Anderson, and R. Gruener. 1980. Changes in synaptic potential properties during acetylcholine receptor accumulation and neurospecific interactions in *Xenopus* nerve muscle cell culture. *Dev. Biol.* 78:464-483.
- Linner, J. G., S. A. Livesey, D. S. Harrison, and A. L. Steiner. 1986. A new technique for removal of amorphous phase tissue water without ice crystal damage: a preparative method for ultrastructural analysis and immunoelectron microscopy. *J. Histochem. Cytochem.* 34:1123-1135.
- Matthews-Bellinger, J., and M. M. Salpeter. 1978. Distribution of acetylcholine receptors at from neuromuscular junctions with a discussion of some physiological implications. *J. Physiol. (Lond.)* 279:197-213.
- Mishina, M., T. Takai, K. Imoto, M. Noda, T. Takahashi, and S. Numa. 1986. Molecular distinction between fetal and adult forms of muscle acetylcholine receptor. *Nature (Lond.)* 321:406-411.
- Ohtake, N. 1986. Attachment of cytoskeletons to cell membranes in human blood platelets as revealed by the quick-freezing and deep-etching replica method. *J. Ultrastruct. Mol. Struct. Res.* 95:84-95.
- Porter, K. R., and K. L. Anderson. 1982. The structure of the cytoplasmic matrix preserved by freeze-drying and freeze-substitution. *Eur. J. Cell Biol.* 29:83-96.
- Post, J. A., A. J. Verkleij, B. Roelofsens, and J. A. F. Op de Kamp. 1988. Plasmalogen content and distribution in the sarcolemma of cultured neonatal rat myocytes. *FEBS (Fed. Eur. Biochem. Soc.) Lett.* 240:78-82.
- Quartararo, N., and P. H. Barry. 1987. A simple technique for transferring excised patches of membrane to different solutions for single channel measurements. *Pflugers Arch. Eur. J. Physiol.* 410:677-678.
- Sakmann, B., and E. Neher. 1983. Geometric parameters of pipettes and membrane patches. In *Single-Channel Recording*. B. Sakmann and E. Neher, editors. Plenum Publishing Corp., New York. 37-51.
- Sargent, P. B., B. E. Hedges, L. Tsavaler, L. Clemmons, S. Tzartos, and J. M. Lindstrom. 1984. Structure and transmembrane nature of the acetylcholine receptor in Amphibian skeletal muscle as revealed by cross-reacting monoclonal antibodies. *J. Cell Biol.* 98:609-618.
- Sokabe, M., and F. Sachs. 1990. The structure and dynamics of patch-clamped membranes: a study of differential interference microscopy. *J. Cell Biol.* 111:599-606.
- Srinivasan, Y., L. Elmer, J. Davis, V. Bennett, and K. Angelides. 1988. Ankyrin and spectrin associate with voltage-dependent sodium channels in brain. *Nature (Lond.)* 333:177-180.
- Steiner, J. P., H. T. Walke, and V. Bennett. 1989. Calcium/calmodulin inhibits direct binding of spectrin to synaptosomal membranes. *J. Biol. Chem.* 264:2783-2791.
- Veltel, D., and H. Robenek. 1988. Immunogold surface replica study on the distribution of acetylcholine receptors in cultured rat myotubes. *J. Histochem. Cytochem.* 36:1295-1303.
- Verkleij, A. J., B. Humbel, D. Studer, and M. Muller. 1985. 'Lipidic particle' systems as visualized by thin-section electron microscopy. *Biochim. Biophys. Acta.* 812:591-594.
- Wall, D. A., and S. Patel. 1989. Isolation of plasma membrane complexes from *Xenopus* oocytes. *J. Membr. Biol.* 107:189-201.